Appl Biochem Biotechnol
https://doi.org/10.1007/s12010-018-2735-1

# Investigation of Binding Affinity Between Prokaryotic Proteins (AHU-IHF) and DNAs: Steered Molecular Dynamics Approach

**Hung Nguyen**[1,2] · **Tri Pham**[1] · **Hoang Linh Nguyen**[1] · **Tuyn Phan**[1]

Received: 25 October 2017 / Accepted: 12 March 2018


**Abstract** The aim of this work is to investigate the binding affinity between the prokaryotic proteins—AHU-IHF proteins (AHU (AHU2, TR3, and AHU6) and IHF (IHF-WT and IHF-βE44A))—and DNAs (DNA, H′-DNA, and H′44A-DNA) by using the steered molecular dynamics (SMD) simulation and the molecular mechanics Poisson-Boltzmann surface area (MM-PBSA) method. The gained results show that although the fluctuation of the pulling force yielded the change of the pulling work, the higher pulling work of the AHU/DNA complexes in comparison to those of the IHF/DNA complexes is not only dependent on the pulling force but also controlled by the change of the trajectory in SMD simulation process. In this study, the pulling work profile not only described the pulling pathway of the complexes but also reflected the hindered process of DNAs when AHU-IHF proteins come out from the binding pocket of DNAs. Additionally, the binding free energy (estimated by the MM-PBSA method) is more confident in giving a true effect to the experimental results in comparison to the pulling force and the pulling work values. These results have also shown a fact that the AHU/DNA complexes were more stable than the IHF/DNA complexes.

**Keywords** AHU proteins (AHU2, TR3, and AHU6) · IHF proteins (IHF-WT and IHF-βE44A) · AHU-IHF proteins, DNAs (DNA, H′-DNA, and H′44A-DNA) · AHU/DNA complexes · IHF/DNA complexes · SMD · MM-PBSA method

✉ Hung Nguyen
hung.nv@icst.org.vn

[1] Institute for Computational Science and Technology (ICST), Ho Chi Minh City, Vietnam

[2] Biomedical Engineering Department, University of Technology, Ho Chi Minh City, Vietnam

Published online: 09 May 2018

## Introduction

IHF and HU are members of a prokaryotic protein family, comprising of 90 residues that bind to DNA and known as histone-like protein; they interacted to DNA minor groove in a sequence-specific (IHF) or non-specific (HU) manner to induce the stability of DNA bending [1–3]. Since bacterial binding proteins have a diverse function, they have been difficult to develop their common function. IHF and HU are commonly referred to as histone-like protein and have several similar biological traits to the eukaryotic histone proteins, which are known to be the most conserved proteins in nature [4–6].

IHF protein from *Escherichia coli* is a small heterodimeric protein (~ 20 kDa) that binds to DNA in a sequence-specific manner and induces a large bend (> 160°). Some specific regions are highly conserved among known IHF binding sites [7–9]. Additionally, previous studies have shown that the binding of wild-type (WT-IHF) is disrupted by a single mutation (T to A) at the center position of a conserved TTR motif. The substitution of βGlu44 by Ala prevented IHF from discriminating between A and T at this position. After that, the crystal structures and relative binding affinities for all combinations of IHF-WT and IHF-βGlu44Ala bound to the WT and mutant DNA. Here, IHF-WT binds the mutant H′44A sequence to two orders of magnitude less tightly. IHF-βGlu44Ala binds H′-DNA with slightly diminished affinity, compared to WT-IHF (~ 5× lower) but fails to discriminate against the mutant DNA sequence [10, 11]. IHF-βGlu44Ala binds both H′-DNA and H′44A-DNA sequences with nearly equal affinity, which is in agreement with challenge-phage assays. The presence of a nick in the substrate DNA had little effect on the relative binding affinity compared to an intact DNA substrate [12, 13]. DNA twist plays a major role in DNA recognition by IHF, and that this geometric parameter is dependent on the dinucleotide step and not on the bound IHF variant [14, 15].

The HU binding site estimated by gel mobility shift experiments is varied, and the mesophilic HU from *Escherichia coli* and *Anabaena* predicted by gel mobility analyses bind from 6 to 10 bp per dimer [16, 17]. The *Anabaena* HU (AHU) was co-crystallized, and diffracting co-crystals can be grown with such oligonucleotides which was a fortuitous result of initial crystallization trials with longer binding sites. These biding sites had been assembled from four separate oligonucleotides to create a doubly nicked IHF binding site [15, 18]. However, a different crystal form appeared sporadically; this form contains only one of the original four oligonucleotides (TR3) [19]. Oligonucleotide AHU2 was designed to explore the effect of the T:T mismatches in TR3, and further improved the reproducibility of crystal growth. In which, AHU6 was designed to improve the reproducibility of crystal packing by removing the two overhanging 3’ Cs and replacing the blunt-ended DNA stacking of the first form with two base pairs [20, 21]. Here, the fact that AHU crystallized with small amounts of TR3 in the presence of higher concentrations of a less-distorted DNA duplex led to strong binding of TR3 duplex prediction to AHU in vitro. The affinity of AHU to TR3 duplex is high; it becomes clear that coupling binding data with relevant structural data could enhance the understanding of the strain induced in DNA upon bending and the structural determinants for binding of AHU and IHF to DNA [22–24].

IHF and AHU play architectural roles in replication initiation, transcription regulation, and site-specific recombination and are associated with bacterial nucleoids [25, 26]. The crystal structure of AHU bound to DNA shows that while underlying proline intercalation and asymmetric charge neutralization mechanism of DNA are similar for AHU and IHF, AHU stabilizes different DNA bend angles (~ 105°–140°) [13, 27]. The two bend angles within a

single-HU complex are not coplanar, and the resulting dihedral angle is consistent with negative supercoiling, and they have multiple influences on transcription and translation in bacterial cells [28]. The AHU/DNA and IHF/DNA structures suggest that sharper bending is correlated with longer DNA binding sites and smaller dihedral angles. The AHU-induced bend may be better modeled as a hinge, not a rigid bend [29]. The ability to induce or stabilize varying bend angle is consistent with AHU-IHF role as an architectural cofactor in many different systems that may require differing geometries, which means AHU-IHF have become paradigms for understanding DNA and indirect readout of sequence [30, 31]. This also reflects that while IHF shows significant sequence specificity, AHU binds preferentially to certain damaged or distorted DNA [32].

In this work, the steered molecular dynamics (SMD) simulation [33–36] and the molecular mechanism Poisson-Boltzmann surface area (MM-PBSA) method [37–39] were used to investigate the binding affinity of bacterial DNA binding proteins (AHU-IHF) to the DNA and its mutant (DNAs). These proteins will be involved in stabilizing the lagging strand and interacting with DNA polymerase. They are also capable of wrapping DNA strands and protecting them from being denatured under extreme environmental conditions. Therefore, the prediction of AHU-IHF activity in binding to DNAs will allow better protection against the viral infection as well as multiple influences on transcription and translation in the bacterial cell.

## Materials and Methods

### Materials

The 3D structures of the AHU/DNA-IHF/DNA complexes were taken from Protein Data Bank (PDB) by PDB entry codes 1P78 (AHU2/DNA), 1P71 (TR3/DNA), 1P51 (AHU6/DNA), 1IHF (IHF-WT/DNA), 1OWG (IHF-WT/H′44A-DNA), 1OWF (IHF-βE44A/H′-DNA), and 1OUZ (IHF-βE44A/H′44A-DNA) [5, 10, 15]. Here, AHU proteins are bound to only DNA while IHF proteins are connected to DNAs (including DNA, H′-DNA, and H′44A-DNA).

### Methods

The simulation processes of complexes were subsequently performed using the AMBER99BSC1 force field [40] implemented in GROMACS 5.1.4 package [41] at absolute temperature 303 K, and the TIP3P water model [42] was also used in all simulation systems. All distance bonds within the proteins were constrained using the linear constrain solver (LINCS) algorithm [43]. The electrostatic and van der Waals interactions were used to depict non-bonded interactions, and the non-bonded interaction pair list was updated every 10 fs using a cutoff of 1.4 nm. The particle mesh Ewald truncation method [44] was used to treat the long-range electrostatic interactions. In order to start from these structures, a short simulation of 2 ns was carried out in the NVT ensemble and then was followed by another 3 ns of NPT simulation. The last configurations of the NPT simulations were then selected to conduct the SMD and typical MD simulation. The leap-frog algorithm [45] was used to integrate the equations of motion with the time step set to 2 femtoseconds (fs) for both the SMD and the typical MD simulations.

*Steered Molecular Dynamics Simulation*

In the SMD simulation [33–36], each of the AHU/DNA-IHF/DNA complexes was placed in a triclinic box of 7 nm × 8 nm × 15 nm to have enough space containing and pulling protein from the binding site of DNAs. Here, the box contained ~22,289 water molecules. The 3D coordinates of the center of the complex were 3.5 nm × 4 nm × 4 nm. The complexes were immersed in a salt solution with a given concentration of 0.10 M of sodium and chloride; then, ~35 and ~60 sodium ions were added to the AHU/DNA-IHF/DNA complexes to neutralize the total charge.

AHU-IHF proteins are forcedly pulled out of the binding site of given DNAs along the route that is specified in advance. The pulling force is measured according to the following equation.

$$F(t) = k\left[vt - \left(\vec{r} - \vec{r}_0\right)\vec{n}\right] \tag{1}$$

Here, $k$ is the force constant, $v$ is the pulling velocity, $\vec{n}$ is the pulling direction normal, and $\vec{r}$ and $\vec{r}_0$ are the position of AHU-IHF proteins at time $t$ and initial time. The equation shows if protein moves forward along the leaving pathway, the $\left(\vec{r} - \vec{r}_0\right)$ will increase and the force will decrease; if the pulling force cannot displace protein, then the force will increase by the increase of $t$. In particular, although a virtual cantilever is moving at the constant velocity $v$ along the biggest $z$ axis of the simulation box, the pulling force was applied to AHU-IHF protein farthest peripheral atoms in the $z$ direction (Fig. 1). During the simulations, the spring constant $k$ value was chosen as 600 kJ/(mol nm$^2$) (approximately 1020 pN/nm), which is a typical value used in atomic force microscope (AFM) experiments [46]. The complete disengagement of AHU-IHF proteins from DNA catalytic site obtained through 5 ns for the AHU/DNA complexes and 3 ns for the IHF/DNA complexes with pulling velocity is set at $v = 0.005$ nm/ps.

Furthermore, to estimate the relative binding affinities of the AHU/DNA-IHF/DNA complexes by the use of the SMD simulation, the pulling work profile is also used to evaluate a

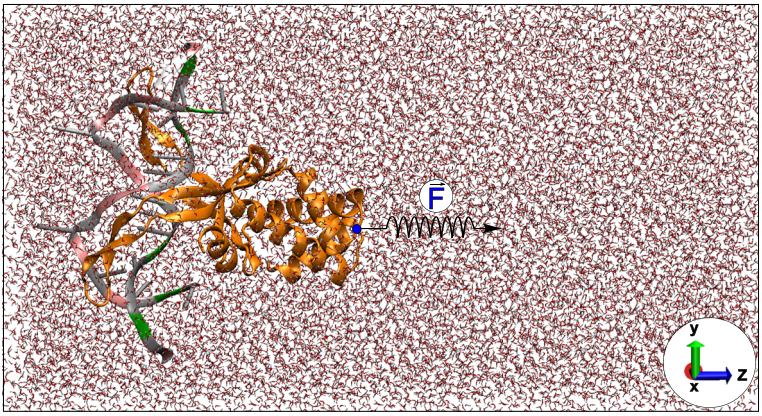


**Fig. 1** The binding position and direction of SMD simulation ($z$ dimension) for the AHU/DNA-IHF/DNA complexes

scoring function to rank the binding affinities of AHU-IHF proteins to DNAs; the pulling work $W_{\text{pull}}$ is approximately defined by the equation.

$$W_{\text{pull}} = \int_0^{r_{\max}} \vec{F}\, \vec{dr} = \int_0^{t_{\max}} \vec{F} \frac{\vec{dr}}{dt} dt \approx \int_0^{t_{\max}} F v dt \approx \sum_{i=1}^{N_{\text{step}}} \frac{(F_{i+1} + F_i)}{2} (r_{i+1} - r_i) \quad (2)$$

where $W_{\text{pull}}$ is the pulling work of external force $F$, and $N_{\text{step}}$ is the total number of step determined in the SMD simulation.

*Binding Free Energy*

In order to determine binding free energy of AHU-IHF proteins to DNAs, the snapshots at equilibrium status of each complex of the typical MD simulation were used to calculate the binding free energy by the use of the MM-PBSA method. The binding free energy of AHU-IHF proteins to DNAs estimated by the MM-PBSA method [37–39] is defined as follows.

$$\Delta G_{\text{bind}} = \Delta E_{\text{elec}} + \Delta E_{\text{vdW}} + \Delta G_{\text{sur}} + \Delta G_{\text{PB}} - T\Delta S \quad (3)$$

Here, $\Delta E_{\text{elec}}$ and $\Delta E_{\text{vdW}}$ are contributions from electrostatic and vdW energies, respectively [47]. $\Delta G_{sur}$ and $\Delta G_{PB}$ are nonpolar and polar solvation energies [48]. The entropic contribution $T\Delta S$ is determined using the normal mode approximation [49].

## Results and Discussion

### Unbinding Process of AHU-IHF Proteins from the Binding Pocket of DNAs

To investigate the binding affinity between AHU-IHF proteins and DNAs, the SMD simulation was used to probe the AHU/DNA-IHF/DNA complexes and to pull AHU-IHF proteins away from the binding site of DNAs, whereby essential energy components involved in the unbinding processes were predicted.

As seen from Fig. 2, the pulling force profile of the AHU/DNA-IHF/DNA complexes is described as a function of simulation time. Here, the rupture force ($F_{\max}$) is a necessary value to break hydrogen bond between AHU-IHF proteins and DNAs. This bonding breaking facilitates AHU-IHF proteins moving from the binding pocket of DNAs, as these complexes are transferred from a stable bound position to unbound state. Specifically, the pulling force profile is able to divide into two consecutive stages: On the one hand, the pulling force continuously increased according to simulation time until AHU-IHF proteins started to dissociate with DNAs, and the external force reached to the rupture force ($F_{\max}$) when the hydrogen bond is broken. On the other hand, the pulling force started to decrease as AHU-IHF proteins moved out from the binding pocket of DNAs in the remaining period.

The fact that the pulling force profile of each complex not only is considered based on the $F_{\max}$ peak but also depends on the time needed for AHU-IHF proteins to come out from the binding pocket of DNAs [33, 50], clearly, the unbinding pathway of the AHU6/DNA complex requires a force $F_{\max} = 993.7$ pN to move out AHU6 from the binding site of DNA; it is larger than the AHU2/DNA complex (at $F_{\max} = 753.4$ pN) and the TR3/DNA complex (at $F_{\max} = 674.6$ pN). This means that the binding affinity of the AHU6/DNA complex is stronger than those of the AHU2/DNA and the TR3/DNA complexes. Similarly, the rupture force of the

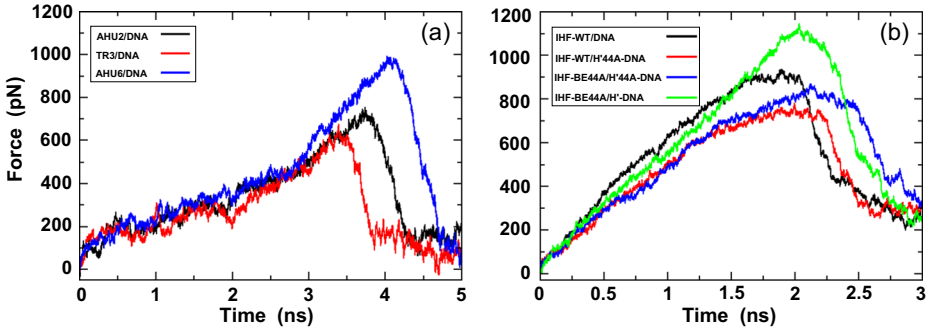


**Fig. 2** The pulling force of the AHU/DNA-IHF/DNA complexes is shown as a function of SMD simulation time

IHF-βE44A/H′-DNA complex (at $F_{max} = 1145.2$ pN) is much larger than that of the IHF-WT/DNA complex (at $F_{max} = 936.5$ pN), the IHF-WT/H′44A-DNA complex (at $F_{max} = 769.3$ pN), and the IHF-βE44A/H′44A-DNA complex (at $F_{max} = 870.6$ pN). This reflected that the IHF-βE44A/H′-DNA complex is much more stable than three remaining complexes. In summary, AHU proteins need ~ 5 ns to come out from the binding pocket of DNA while it needs only ~ 3 ns for IHF proteins to go out from the binding site of DNAs. This may suggest that the binding affinity of the AHU/DNA complexes is better than those of the IHF/DNA complexes.

In another result, in order to evaluate a scoring function to rank the binding affinities of AHU-IHF proteins to DNAs, the pulling work profile of the AHU/DNA-IHF/DNA complexes is also described as in Fig. 3. Here, the pulling work is able to divide in two cases: Firstly, the pulling work of the AHU/DNA-IHF/DNA complexes is extended and obtained maximum value to two sides of ~ [− 75, 75] kcal/mol around 4e + 4 steps for the IHF/DNA complexes and ~ [− 125, 125] kcal/mol around 8e + 4 steps for the AHU/DNA complexes. After that, the pulling work is narrowed to ~ [− 25, 25] kcal/mol in the remaining steps for both kinds of the AHU/DNA-IHF/DNA complexes. The negative value of the pulling work is described as the work part of obstructing force in the process of AHU-IHF proteins and moved out from the binding site of DNAs. This is clear that DNAs have tended to hinder AHU-IHF proteins to come out from its binding site and have simultaneously generated negative values of $(r_{i+1} - r_i)$ and external force $F$. Interestingly, the fluctuation of the pulling force profile according to simulation time (Eq. 1) can yield the change of the pulling work according to the total number of steps (Eq. 2), leading to the higher pulling work of the AHU/DNA complexes in comparison to those of the IHF/DNA complexes. Generally, this result expressed that the pulling work profile not only explained the pulling pathway of these complexes but also described the hindered process of DNAs when AHU-IHF proteins come out from its binding pocket.

In order to monitor the effect of non-bond interactions to the change of the binding affinity of the complexes, the contribution of electrostatic and vdW and interaction energies is also used (Fig. 4). Specifically, at 0 ns, the vdW energy is fluctuated ~ − 175 kcal/mol for the AHU/DNA complexes; meanwhile, it is achieved to ~ − 250 kcal/mol for the IHF/DNA complexes (Fig. 4a, b). Similar to the vdW energy, the electrostatic energy is fluctuated ~ − 3200 kcal/mol for the AHU/DNA complexes while it is decreased to ~ − 5500 kcal/mol for the IHF/DNA complexes (Fig. 4c, d). In unbound process of these complexes, the vdW reached ~ − 25 kcal/mol for AHU proteins and ~ [− 175, − 100] kcal/mol for IHF proteins while the electrostatic

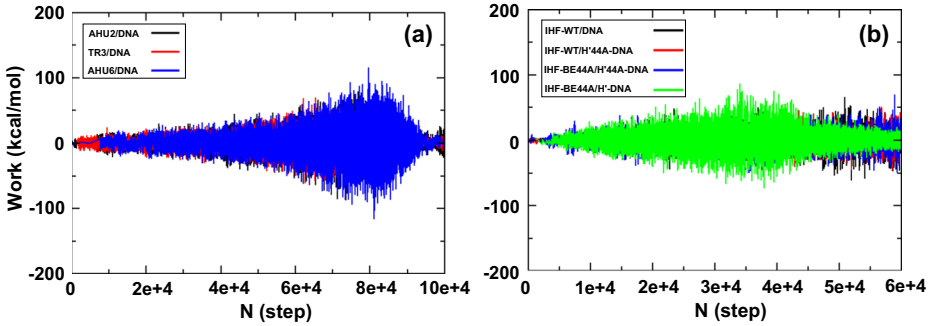


**Fig. 3** The pulling work of the AHU/DNA-IHF/DNA complexes is shown as a function of total number of step (*N* (step))

energy reached ~ − 1000 kcal/mol for AHU proteins and ~ − 4000 kcal/mol for IHF proteins, with AHU-IHF proteins being really separated from DNAs. Additionally, the change of interaction energy (sum of the vdW and electrostatic energies—Fig. 4e, f) is not significantly different in comparison to the electrostatic energy values (Fig. 4e, f). This is clearly shown that the contribution of the electrostatic energy has a more important role in the change of the binding affinity of the AHU/DNA-IHF/DNA complexes in comparison to the vdW energy. In other words, the electrostatic energy of the IHF/DNA complexes is much smaller than that of the AHU/DNA complexes; this could be explained by a different distribution of positive charge of total charge ~ 60 e for the IHF/DNA complexes and ~ 35 e for the AHU/DNA complexes. Generally, this result implied the substantial changes in the contribution of charge which generated significantly different values of the electrostatic energy by affecting strong Coulomb interactions.

The number of contact (NC) ($r < 0.6$ nm) and the number of hydrogen bond (H-bond) ($r < 0.35$ nm) formed between AHU-IHF proteins and DNAs as a function of simulation time (Fig. 5) were used to describe the unbinding process of AHU-IHF proteins from the binding pocket of DNAs. In particular, at the stable bound state, only ~ 10e + 3 NCs are formed for the AHU/DNA complexes while it gained ~ 13e + 3 NCs for the IHF/DNA complexes (Fig. 5a, b). At the unbound state, the NC decreased to ~ 2e + 3 NCs for the AHU/DNA complexes and ~ [6e + 3, 11e + 3] NCs. The same with the NC value, the H-bond value has also shown the unbinding process of the AHU/DNA-IHF/DNA complexes from the bound state to the unbound state (Fig. 5c, d). In more detail, at the bound state, only ~ 20 H-bonds are formed between DNA and AHU proteins while it reached ~ 35 H-bonds for the IHF/DNA complexes. At the unbound state, the H-bond decreased to ~ 5 H-bonds for the AHU/DNA complexes; meanwhile, it fluctuated between ~ [10, 29] H-bonds. Overall, the difference of the NC and H-bond of the AHU/DNA complexes in comparison to that of the IHF/DNA complexes has shown the diverse effect between sequence-specific (IHF) and non-specific (AHU) proteins. Additionally, the decrease of the NC and H-bond of the TR3/DNA complexes in comparison to those of the AHU2/DNA and AHU6/DNA complexes is caused by the effect of the T:T mismatches in TR3. Generally, although the NC and H-bond networks of AHU proteins bound to DNA are less than IHF proteins bound to DNAs, the binding affinity of the AHU/DNA complexes seems to be stronger than that of the IHF/DNA complexes. This is caused by the fluctuation of the entropy values described below.

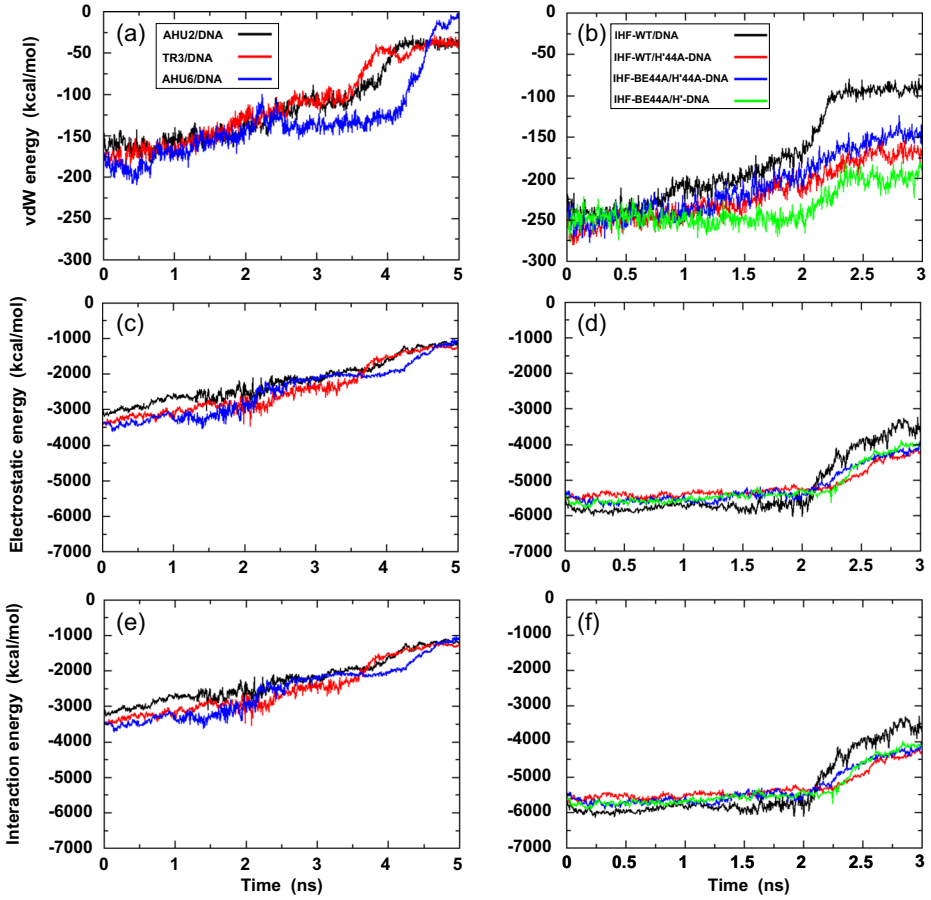


**Fig. 4** The vdW and electrostatic and total energies of the AHU/DNA-IHF/DNA complexes are illustrated as a function of SMD simulation time

## The Binding Affinity Between DNAs and AHU-IHF Proteins

In order to investigate the binding affinity of the AHU/DNA-IHF/DNA complexes, in addition to the pulling force and the pulling work profiles, the binding free energy ($\Delta G$) estimated by the MM-PBSA method is also used to evaluate the complex's stability as well as the binding mechanism of AHU-IHF proteins to the binding pocket of DNAs. As shown in Table 1, the contribution of different energy components in determining the $\Delta G$ expressed that the electrostatic energy ($\Delta E_{\text{elec}}$) has a more important role than the vdW energy ($\Delta E_{\text{vdW}}$). The changes of the nonpolar solvation energy ($\Delta G_{\text{sur}}$) values are not an important contribution to the difference of the $\Delta G$ among the complexes. The entropy ($T\Delta S$) of the IHF/DNA complexes is almost double in comparison with those of the AHU/DNA complexes. The loss of polar solvation energy ($\Delta G_{\text{PB}}$) is compensated by the remaining components of the $\Delta G$ in these simulation systems.

Specifically, the $\Delta E_{\text{elec}}$ achieved from the complex formation compensates which begins by the loss in the $\Delta G_{\text{PB}}$. Here, the $\Delta E_{\text{elec}}$ of the IHF/DNA complexes (ranged from − 5560.9 to − 5449.2 kcal/mol) seem to be twice larger as that of the AHU/DNA complexes (ranged

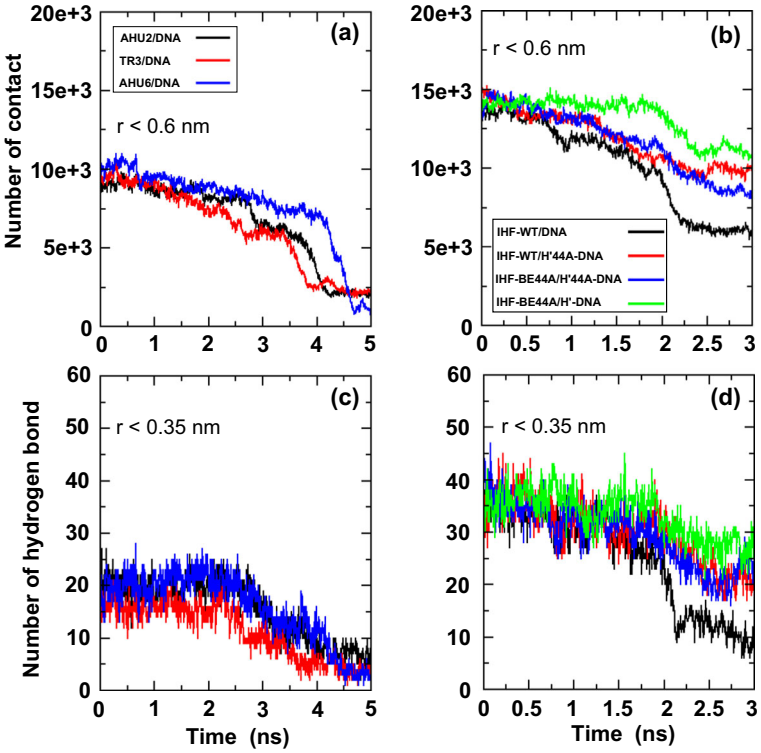


**Fig. 5** The number of contact (**a**) and the number of hydrogen bond (**b**) formed between DNAs and AHU-IHF proteins are presented as a function of SMD simulation time

from − 3409.4 to − 2710.6 kcal/mol). While the $\Delta E_{vdW}$ of the AHU/DNA complexes (ranged from − 167.6 to − 151.3 kcal/mol) and the IHF/DNA complexes (ranged from − 252.2 to − 214.1 kcal/mol) contribute significantly to the difference of the $\Delta G$; the $\Delta G_{sur}$ of all complexes (ranged from − 8.2 to − 5.5 kcal/mol) does not lead to the change of the $\Delta G$. The $T\Delta S$ of the AHU/DNA complexes (fluctuated between 23.2 and 28.3 kcal/mol) are nearly twice smaller as compared to those of the IHF/DNA complexes (fluctuated between 42.5 and

**Table 1** The binding free energies (kcal/mol) of the AHU/DNA-IHF/DNA complexes estimated by the MM-PBSA method. The rupture force—$F_{max}$ (pN)—and the maximum pulling work—$W_{max}$ (kcal/mol)—determined from the data of the SMD simulation

| Values<br>Complexes | $\Delta E_{elec}$ | $\Delta E_{vdW}$ | $\Delta G_{sur}$ | $\Delta G_{PB}$ | $-T\Delta S$ | $\Delta G_{bind}$ | $F_{max}$ | $W_{max}$ |
|---|---|---|---|---|---|---|---|---|
| AHU2/DNA | − 2793.6 | − 158.2 | − 6.4 | 2853.6 | 28.3 | − 74.3 | 753.4 | 76.3 |
| TR3/DNA | − 2710.6 | − 151.3 | − 5.5 | 2770.5 | 23.2 | − 71.7 | 674.6 | 70.7 |
| AHU6/DNA | − 3409.4 | − 167.6 | − 7.1 | 3480.4 | 23.4 | − 78.3 | 993.7 | 113.4 |
| IHF-WT/DNA | − 5529.8 | − 214.1 | − 8.2 | 5652.3 | 51.7 | − 48.1 | 936.5 | 71.4 |
| IHF-WT/H′44A-DNA | − 5560.9 | − 234.6 | − 8.0 | 5731.8 | 44.1 | − 27.6 | 769.3 | 50.5 |
| IHF-βE44A/H′44A-DNA | − 5449.2 | − 232.1 | − 7.7 | 5592.9 | 50.3 | − 45.8 | 870.6 | 73.3 |
| IHF-βE44A/H′-DNA | − 5511.7 | − 252.2 | − 7.3 | 5666.5 | 42.5 | − 62.2 | 1145.2 | 91.2 |

51.7 kcal/mol); it is clearly reflected that the fluctuation of the IHF/DNA complexes is more chaotic than those of the AHU/DNA complexes. Finally, the $\Delta G$ of the IHF/DNA complexes (the $\Delta G_{\text{bind}}$ being from −62.2 to −27.6 kcal/mol) is lower than those of the AHU/DNA complexes (the $\Delta G_{\text{bind}}$ going from −78.3 to −71.7 kcal/mol); this confirms that the AHU/DNA complexes are more stable than the IHF/DNA complexes. In more detail, for the AHU/DNA complexes, the $\Delta G$ of the AHU6/DNA complex is smaller than that of the AHU2/DNA and TR3/DNA complexes, as an evidence that AHU6 bound to DNA is stronger in comparison to AHU2 and TR3 proteins. For the IHF/DNA complexes, the $\Delta G$ of the IHF-βE44A/H′-DNA complex is much higher in comparison to those of the three IHF's remaining complexes, in which, the difference of the $\Delta$G among three remaining complexes is not significant. This is caused by the contribution of DNA twist which played a key role in DNA recognition; this geometric parameter is dependent on the dinucleotide step and not on the bound IHF variant [15] in estimating the $\Delta G$.

In summary, the difference of the binding affinity of the AHU/DNA complexes is caused by only the change of AHU proteins (AHU2, TR3, and AHU6) while it depended on the dinucleotide step of DNA twist and not on the bound of IHF variant in the IHF/DNA complexes. The gained results of the $\Delta G$, the $F_{\max}$, and the $W_{\max}$ are shown in good agreement with the experimental results [7, 18]. Here, the $\Delta G$ is even more confident in giving a true effect to the experimental results in comparison to the $F_{\max}$ and the $W_{\max}$. From the gained results, this finding also reflected a fact that DNAs are expected to yield a more stable complex with AHU proteins more than with IHF proteins.

## Conclusions

In this study, we applied the SMD simulation and the MM-PBSA method to investigate the unbinding process and the binding affinity of the AHU/DNA-IHF/DNA complexes. A number of interesting results are shown as follows.

(i) Although the fluctuation of the pulling force yielded the change of the pulling work, the higher pulling work of the AHU/DNA complexes in comparison to those of the IHF/DNA complexes is not only dependent on the pulling force but also controlled by the change of the trajectory in the SMD simulation process. Additionally, the pulling work not only explained the pulling pathway of these complexes but also reflected the hindered process of DNAs when AHU-IHF proteins come out from the binding pocket of DNAs.

(ii) The difference of the NC and the H-bond between the AHU/DNA-IHF/DNA complexes describes the diverse effect between sequence-specific (IHF) and non-specific (AHU) proteins. Although the NC and the H-bond of the AHU/DNA complexes are less than in comparison to those of the IHF/DNA complexes, the entropy result estimated from the MM-PBSA method has shown a fact that DNAs seem to be a more stable complex with AHU proteins than with IHF proteins.

(iii) The $\Delta G$, the $F_{\max}$, and the $W_{\max}$ values are in good agreement with the experimental results. Here, the $\Delta G$ is even more confident to give a true effect to the experimental results in comparison to the $F_{\max}$ and the $W_{\max}$. The gained results confirm that DNAs are expected to yield a more stable complex with AHU proteins more than with IHF proteins.

**Acknowledgments** We sincerely thank Prof. Mai Suan Li from the Institute of Physics, Polish Academy of Science, Poland, for the support and valuable comments. The computing resources were provided by the HPC Lab of HCMC University of Technology.

**Author Contributions** Hung Nguyen designed the research, carried out the simulations, analyzed the data, and wrote the manuscript. Hoang Linh Nguyen, Tri Pham, and Tuyn Phan analyzed the data. All authors have seen, read, and approved the manuscript.

**Funding Information** This research was funded by the Department of Science and Technology – Ho Chi Minh City (HCMC – DOST), and the Institute for Computational Science and Technology (ICST) at Ho Chi Minh City, Vietnam, under Contract No. 27/2017/HD-KHCNTT.

## Compliance with Ethical Standards

**Competing Interest** The authors declare that they have no competing interests.

## References

1. Drlica, K., & Rouviere-Yaniv, J. (1987). Histone like proteins of bacteria. *Microbiological Reviews, 51*(3), 301–319.
2. Pettijohn, D. E. (1988). Histone-like proteins and bacterial chromosome structure. *Journal of Biological Chemistry, 263*(26), 12793–12796.
3. Hamidon, N. H., Suraiya, S., Sarmiento, M. E., Acosta, A., Norazmi, M. N., & Lim, T. S. (2017). Immune TB antibody phage display library as a tool to study B cell immunity in TB infections. *Applied Biochemistry and Biotechnology, 184*(3), 852–868.
4. Griffith, A. J. F., Wessler, S. R., Carroll, S. B., & Doebley, J. *An introduction to genetic analysis* (10th ed.pp. 428–429). New York: W. H. Freeman and Company.
5. Wojtuszewski, K., Hawkins, M. E., Cole, J. L., & Mukerji, I. (2001). HU binding to DNA: evidence for multiple complex formation and DNA bending. *Biochemistry, 40*(8), 2588–2598.
6. Monu, & Meena, L. S. (2016). Roles of triolein and lipolytic protein in the pathogenesis and survival of *Mycobacterium tuberculosis:* a novel therapeutic approach. *Applied Biochemistry and Biotechnology, 178*(7), 1377–1389.
7. Mouw, K. W., & Rice, P. A. (2007). Shaping the Borrelia burgdorferi genome: crystal structure and binding properties of the DNA-bending protein Hbb. *Molecular Microbiology, 63*(5), 1319–1330.
8. Lorenz, M., Hillisch, A., & Diekmann, S. (2002). Fluorescence resonance energy transfer studies of U-shaped DNA molecules. *Reviews in Molecular Biotechnology, 82*(3), 197–209.
9. Chen, L., Guo, S., Wu, L., Fan, X., Ma, H., Wu, K., Wu, J., & Zhang, J. (2015). IL-17A autoantibody induced by recombinant *Mycobacterium smegmatis* expressing Ag85A-IL-17A fusion protein. *Applied Biochemistry and Biotechnology, 176*(7), 2018–2026.
10. Yang, C. C., & Nash, H. A. (1989). The interaction of E. coli IHF protein with its specific binding sites. *Cell, 57*(5), 869–880.
11. Kumari, P., & Meena, L. S. (2014). Factors affecting susceptibility to *Mycobacterium tuberculosis*: a close view of immunological defence mechanism. *Applied Biochemistry and Biotechnology, 174*(8), 2663–2673.
12. Sharma, S., & Meena, L. S. (2017). Potential of $Ca^{2+}$ in *Mycobacterium tuberculosis* $H_{37}$Rv pathogenesis and survival. *Applied Biochemistry and Biotechnology, 181*(2), 762–771.
13. Sorek, R., Lawrence, C. M., & Wiedenheft, B. (2013). CRISPR-mediated adaptive immune systems in bacteria and archaea. *Annual Review of Biochemistry, 82*(1), 237–266.
14. Boelens, R., Vis, H., Vorgias, C. E., Wilson, K. S., & Kaptein, R. (1996). Structure and dynamics of the DNA binding protein HU from Bacillus stearothermophilus by NMR spectroscopy. *Biopolymers, 40*(5), 553–559.
15. Lynch, T. W., Read, E. K., Mattis, A. N., Gardner, J. F., & Rice, P. A. (2003). Integration host factor: putting a twist on protein-DNA recognition. *Journal of Molecular Biology, 330*, 493–502.
16. Broyles, S. S., & Pettijohn, D. E. (1986). Interaction of the Escherichia coli HU protein with DNA. Evidence for formation of nucleosome like structures with altered DNA helical pitch. *Journal of Molecular Biology, 187*(1), 47–60.

17. Bonnefoy, E., & Rouviere-Yaniv, J. (1991). HU and IHF, two homologous histone-like proteins of Escherichia coli, form different protein-DNA complexes with short DNA fragments. *The EMBO Journal, 10*(3), 687–696.
18. Swinger, K. K., Lemberg, K. M., Zhang, Y., & Rice, P. A. (2003). Flexible DNA bending in HU-DNA cocrystal structures. *The EMBO Journal, 22*(14), 3749–3760.
19. Nagaraja, R., & Haselkorn, R. (1994). Protein HU from the cyanobacterium Anabaena. *Biochimie, 76*(10-11), 1082–1089.
20. Yang, S. W., & Nash, H. A. (1995). Comparison of protein binding to DNA in vivo and in vitro: defining an effective intracellular target. *The EMBO Journal, 14*(24), 6292–6300.
21. Dang, G., Chen, L., Li, Z., Deng, X., Cui, Y., Cao, J., Yu, S., Pang, H., & Liu, S. (2015). Expression, purification and characterisation of secreted esterase Rv2525c from Mycobacterium tuberculosis. *Applied Biochemistry and Biotechnology, 176*(1), 1–12.
22. Shindo, H., Furubayashi, A., Shimizu, M., Miyake, M., & Imamoto, F. (1992). Preferential binding of E. coli histone-like protein HU alpha to negatively supercoiled DNA. *Nucleic Acids Research, 20*(7), 1553–1558.
23. Nash, H. A. (1996). The HU and IHF proteins: accessory factors for complex protein-DNA assemblies. In E. C. C. Lin & A. S. Lynch (Eds.), *Regulation of gene expression in Escherichia coli* (pp. 150–179). Austin: R. G. Landes Co..
24. Swinger, K. K., & Rice, P. A. (2006). Structure-based analysis of HU-DNA binding. *Journal Molecular Biology, 365*, 1005–1016.
25. Kim, D. H., Im, H., Jee, J. G., Jang, S. B., Yoon, H. J., Kwon, A. R., Kang, S. M., & Lee, B. J. (2014). β-Arm flexibility of HU from Staphylococcus aureus dictates the DNA-binding and recognition mechanism. *Acta Crystallographica Section D: Structural Biology, 70*(12), 3273–3289.
26. Lorenz, M., Hillisch, A., Goodman, S. D., & Diekmann, S. (1999). Global structure similarities of intact and nicked DNA complexed with IHF measured in solution by fluorescence resonance energy transfer. *Nucleic Acids Research, 27*(23), 4619–4625.
27. Grove, A. (2011). Functional evolution of bacterial histone-like HU proteins. *Current Issues in Molecular Biology, 13*(1), 1–12.
28. Tan, C., Terakawa, T., & Takada, S. (2016). Dynamic coupling among protein binding, sliding, and DNA bending revealed by molecular dynamics. *Journal of the American Chemical Society, 138*(27), 8512–8522.
29. Vivas, P., Kuznetsov, S. V., & Ansari, A. (2008). New insights into the trasition pathway from nonspecific to specific complex of DNA with *Escherichia Coli* integration host factor. *The Journal of Physical Chemistry B, 112*(19), 5997–6007.
30. Christodoulou, E., Rypniewski, W. R., & Vorgias, C. E. (2003). High-resolution X-ray structure of the DNA-binding protein HU from the hyper-thermophilic *Thermotoga maritime* and the determinants of its thermostability. *Extremophiles, 7*(2), 111–122.
31. Kamashex, D., Balandina, A., & Roviere-Yaniv, J. (1999). The binding motif recognized by HU on both nicked and cruciform DNA. *The EMBO Journal, 18*(19), 5434–5444.
32. Ghosh, S., & Grove, A. (2004). Histone-like protein HU from Deinococcus radiodurans binds preferentially to four-way DNA junctions. *Journal of Molecular Biology, 337*(3), 561–571.
33. Nguyen, H., & Le, L. (2015). Steered molecular dynamics approach for promising drugs for influenza A virus targeting channel proteins. *European Biophysics Journal, 44*(6), 447–455.
34. Nguyen, H., Tran, T., Fukunishi, Y., Higo, J., Nakamura, H., & Le, L. (2015). Computational study of drug binding affinity to influenza A Neuraminidase using smooth reaction path generation (SRPG) method. *Journal of Chemical Information and Modeling, 55*, 1936–1943.
35. Nguyen, H., Do, N., Phan, T., & Pham, T. (2018). Steered molecular dynamics for investigating the interactions between insulin receptor tyrosine kinase (IRK) and variants of protein tyrosine phosphatase 1B (PTP1B). *Applied Biochemistry and Biotechnology, 184*(2), 401–413.
36. Vuong, Q. V., Nguyen, T. T., & Li, M. S. (2015). A new method for navigating optimal direction for pulling ligand from binding pocket: application to ranking binding affinity by steered molecular dynamics. *Journal of Chemical Information and Modeling, 55*(12), 2731–2738.
37. Nguyen, H., Nguyen, T., & Le, L. (2016). Computational study of glucose-6-phophate-dehydrogenase deficiencies using molecular dynamics simulation. *South Asian Journal of Life Sciences, 4*(1), 32–39.
38. Nguyen, T. T., Mai, B. K., & Li, M. S. (2011). Study of Tamiflu sensitivity of variants of A/H5N1 virus using different force fields. *Journal of Chemical Information and Modeling, 51*(9), 2266–2276.
39. Huy, P. D. Q., & Li, M. S. (2014). Binding of fullerenes to amyloid beta fibrils: size matters. *Physical Chemistry Chemical Physics, 16*(37), 20030–20040.
40. Ivani, I., Dans, P. D., Noy, A., Pérez, A., Faustino, I., Hospital, A., Walther, J., Andrio, P., Goñi, R., Balaceanu, A., Portella, G., Battistini, F., Gelpí, J. L., González, C., Vendruscolo, M., Laughton, C. A., Harris, S. A., Case, D. A., & Orozco, M. (2016). Parmbsc1: a refined force field for DNA simulations. *Nature Methods, 13*(1), 55–58.

41. Hess, B., Kutzner, C., van der Spoel, D., & Lindahl, E. (2008). GROMACS 4: algorithms for highly efficient, load-balanced, and scalable molecular simulation. *Journal of Chemical Theory and Computation, 4*(3), 435–447.
42. Mark, P., & Nilsson, L. (2001). Structure and dynamics of the TIP3P, SPC, and SPC/E water models at 298 K. *The Journal of Physical Chemistry A, 105*(43), 9954–9960.
43. Hess, B., Bekker, H., Berendsen, H. J. C., & Fraaije, J. G. E. M. (1997). LINCS: a linear constraint solver for molecular simulations. *Journal of Computational Chemistry, 18*(12), 1463–1472.
44. Darden, T., York, D., & Pedersen, L. (1993). Particle mesh Ewald: an *N* log(*N*) method for Ewald sums in large systems. *The Journal of Chemical Physics, 98*(12), 10089–10092.
45. Hockney, R. W., Goel, S. P., & Eastwood, J. (1974). Quit high resolution computer models of plasma. *Journal of Computational Physics, 14*(2), 148–158.
46. Gibson, C. T., Carnally, S., & Roberts, C. J. (2007). Attachment of carbon nanotubes to atomic force microscope probes. *Ultramicroscopy, 107*(10-11), 1118–1122.
47. Baker, N. A., Sept, D., Joseph, S., Holst, M. J., & McCammon, J. A. (2001). Electrostatics of nanosystems: application to microtubules and the ribosome. *Proceedings of the National Academy of Science of the United States America, 98*(18), 10037–10041.
48. Binnig, G., Quate, C. F., & Gerber, C. (1986). Atomic force microscope. *Physical Review Letters, 56*, 1196.
49. Duan, L., Liu, X., & Zhang, J. Z. (2016). Interaction entropy: a new paradigm for highly efficient and reliable computation of protein-ligand binding free energy. *Journal of the American Chemical Society, 138*(17), 5722–5728.
50. Nguyen, H., Nguyen, H. L., Linh, H. Q., & Nguyen, M. T. (2018). Binding affinity of the L-742,001 inhibitor to the endonuclease domain of A/H1N1/PA influenza virus variants: molecular simulation approaches. *Chemical Physics, 500*, 26–36.